

Investigation effect of benzotriazole on the corrosion of brass-MM55 alloy in artificial seawater by dynamic EIS

Husnu Gerengi · Kazimierz Darowicki · Pawel Slepki ·
Gozen Bereket · Jacek Ryl

Received: 4 March 2009 / Revised: 11 August 2009 / Accepted: 12 August 2009 / Published online: 16 September 2009
© Springer-Verlag 2009

Abstract The electrochemical behavior of brass-MM55 alloy was studied in artificial seawater with benzotriazole by using a novel method called dynamic electrochemical impedance spectroscopy (DEIS). This method gives possibility to investigate the protection of metals in corrosive medium by using inhibitors in galvanostatic conditions for a long time. Instantaneous impedance spectra for brass-MM55 were recorded for 10 h in artificial seawater for different concentration of benzotriazole. It was found that a few hours were not enough for the accurate calculation of corrosion inhibition. Also with this method it is possible to figure out how the charge transfer resistance (R_{ct}) changes by the time. Usefulness of the DEIS technique in the investigation of non-stationary phenomena has been proved in the field of inhibitor research. All studies clearly show that benzotriazole inhibits the corrosion of brass-MM55 alloy in artificial seawater solution and the value of inhibition efficiency increases with increasing concentration of benzotriazole.

“Presented at the international conference “Corrosion Today” held in Gdansk-Sobieszewo, Poland, 23 to 26 April 2008.”

H. Gerengi (✉)
Department of Chemistry, Kaynasli Vocational College,
Duzce University,
81900 Kaynasli-Duzce, Turkey
e-mail: husnugerengi@duzce.edu.tr

K. Darowicki · P. Slepki · J. Ryl
Department of Electrochemistry, Corrosion and Material
Engineering, Gdansk University of Technology,
Narutowicza Str. 11/12,
80-233 Gdansk, Poland

G. Bereket
Department of Chemistry, Faculty of Arts and Science,
Eskisehir Osmangazi University,
26480 Eskisehir, Turkey

Keywords Corrosion · Artificial seawater · Brass-MM55 · Benzotriazole (BTA) · Dynamic electrochemical impedance spectroscopy (DEIS)

Introduction

Copper and its alloys are widely used in industry because of their excellent electrical and thermal conductivity and are often used in heating and cooling systems [1, 2]. Especially, brass has been widely used as tubing material for condensers and as heat exchanger in various cooling water systems [3, 4]. Due to those various industrial applications and economic importance of brass, its protection against corrosion attracted much attention. However, it corrodes easily in chloride containing aqueous solutions and air, which limits its use. But the majority of marine propellers from the smallest to the largest are made from copper alloys [5]. Brass-MM55 has been especially used as casting propeller and as rudder [6]. This type of brass has also been used in valve bodies, pump parts, and non-magnetic binnacle fittings [7].

One of the most important methods in corrosion protection is to use inhibitors [8–10]. Inhibitors are chemicals that act to slow down corrosion. They are the preferred method of corrosion control in closed and recirculation cooling and heater systems. The effectiveness of an organic substance as an inhibitor depends on the structure of the inhibitor [11] and the stability of the chelate formed on the metal surface [12]. Most organic substances employed as copper corrosion inhibitors protect the metal by forming a chelate on the metal surfaces [13]. Benzotriazole (BTA) is known as one of the best corrosion inhibitors for copper and its alloys in a wide range of environments [14–18]. Also BTA has low toxicity and

presents no ecological hazard although precautions should be taken [19]. It is generally assumed that BTA forms a polymeric cuprous complex on the metal surface which prevents further copper dissolution [20, 21]. Most of above studies concerned that BTA adsorbed on the copper alloys surface according to reaction (1).



Brass has been widely studied in 3.5% NaCl media where it has been observed that the chloride ion has a strong influence on the copper corrosion mechanism [22]. However, according to laboratory tests, these solutions do not always reproduce the corrosion accurately losses in the natural seawater, because, in addition to chlorides, other impurities in the salt composition can pronouncedly affect the corrosion [23].

Darowicki et al. [24, 25] have presented a new mode of electrochemical impedance measurement. In this method (dynamic electrochemical impedance spectroscopy (DEIS)), the impedance spectra are determined for narrow periods of time. The purpose of this work is to present a novel method, dynamic electrochemical impedance spectroscopy, which has never been employed in the investigation of protection of metals by adding inhibitor to corrosive medium.

Experimental approach

Materials

Electrochemical measurements were all carried out at room temperature, in a three-electrode type cell with separate compartments for the reference electrode (Ag/AgCl) and the counter electrode was platinum (Pt) plate. During the all measurements, the solution was stirred with magnetic bar (500 rot/min). The working electrode was brass-MM55. The area of this electrode was 0.2 cm² and surface of the working electrode was prepared by grinding abrasive paper of 400–1,800 gradation. Next, they were rinsed with distilled water and degreased with acetone. In each experiment, after 10 min of the beginning of the experiment, we added BTA (Roanal Ltd. Hungary, product number: 02070). Thus, we investigated how BTA acted on our sample. Brass-MM55 had the composition 55% Cu, 4% Mn, 1% Fe, 0.6% Al, and the rest Zn. Chemical composition of the artificial seawater is given in Table 1 [26]. pH of our solution was 8.10 and resistivity was (ρ) 25 Ω cm. The conductivity was measured by Nilsson electrical resistance conductance meter model 400.

Table 1 Composition of the artificial seawater

Component	Concentrations, g/l
NaCl	24.530
MgCl ₂	5.200
Na ₂ SO ₄	4.090
CaCl ₂	1.160
NaHCO ₃	0.201
KBr	0.101
H ₃ BO ₃	0.027

Method

Dynamic electrochemical impedance spectroscopy technique is the perturbation of a multi-sine signal. A system under investigation is perturbed with a set of sine voltage or current signals having the same amplitude but different frequencies. This method is general and allows the analysis of impedance spectra in a joint time–frequency domain. The perturbation and response signals are registered continuously during the measurement. The analyzing window function is employed to cut a fragment out of the recorded register. In the next step this segment is subjected to the regular Fourier transformation and an instantaneous spectrum is determined. The spectrum is averaged over the time range equal to the length of the analyzing window [27].

Generation of the current was performed with a National Instruments Ltd. PCI-6120 digital–analog card. The same card was used to measure the current and voltage signals. Autolab PGSTAT 30 equipment was used to supply galvanostatic condition and also, as a current–voltage converter. The perturbation signal was a package composed of 20 elementary current sinusoids of the frequency range 4.5 kHz to 700 mHz. Logarithmic distribution of frequencies of excitation signal was chosen due to best representation of impedance variations on such scale.

Two criteria were taken into consideration in selection of amplitudes. First of them was increase of potential response together with drop of signal frequency for impedance measurements in galvanostatic mode. To allow proper detection of resultant signal in the range of all applied frequencies diminished amplitudes were used for low-frequency elementary signals. Increase of system impedance while an experiment proceeds was second issue taken into consideration during formation of the perturbation signal. Perturbation amplitudes were selected in such a way to assure that resultant response signal peak-to-peak amplitude will not exceed 10 mV at any stage of experiment.

Lowest frequency of perturbation signal determines the size of analyzing window, which in this particular case was 10 s. It means that each and every impedance spectra

achieved represent averaged value of impedance from the time period of 10 s. On the other side, highest frequency range determines the sampling frequency, which was equal to 12.5 kHz in this case. Detailed information regarding dynamic EIS measurements carried out in galvanostatic mode was presented by Slepski et al. [28].

Results and discussion

Ten minutes after starting each DEIS experiment, the required amount of BTA (e.g. to have the determined concentration of BTA in artificial seawater) was added quickly to the corrosion cell. Without and with the inhibitors (Fig. 1) 0.0100 M, 0.0134 M, 0.0201 M, and 0.0268 M BTA, DEIS results were depicted in Figs. 1, 2, 3, 4, and 5.

Individual impedance spectra presented in the form of Nyquist plot manifest shape of flattened semicircles in the high frequency range, magnitude of which increases. Changes of shape of impedance spectra are also visible in the range of low frequencies where they form straight line. It should be noted, that for every experiment changes of impedance spectra are most visible for the first few hours of exposition. Afterwards, one can say that the investigated system has stabilized. For proper construction of the electric equivalent circuit one has to take into consideration both the structure of analyzed system and the processes occurring within it. Exposition of the electrode to NaCl solution leads to formation of surface layer mostly composed of ZnO with the addition of Cu₂O and others [29–31]. Presence of BTA in the electrolyte entirely changes the composition of such a layer. As a result of chemisorptions, a compact layer is formed which is composed of Cu(I)BTA and Zn(II)BTA complexes with the addition of adequate oxides that effectively limits further corrosion process. Electric equivalent circuit should

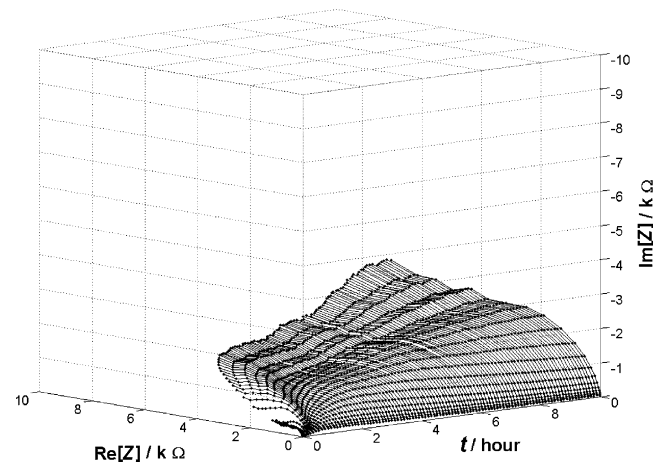


Fig. 2 DEIS result of Brass-MM55 with 0.0100 M BTA in artificial seawater

also contain elements representing electrode process, charge transfer resistance, and double layer capacitance as well as elements representing transport of reagents.

In previous research, impedance spectra obtained on brass in the presence of BTA are effectively analyzed with the use of simple electric equivalent circuit consisting of solution resistance, charge transfer resistance, and constant phase element (CPE) connected with electric double layer capacitance [32] or taking into consideration differences for low- and high-frequency region [33, 34]. Kosec et al. [29] have introduced second time constant (RQ) representing influence of surface layer in electric equivalent circuit. This time constant was observed in the area of highest frequencies ranging up to kHz. Resultant values of analyzed circuit elements were considerably lower in respect to charge transfer resistance and CPE representing electric double layer capacitance. This can explain omission of such surface layer in impedance data analysis presented by other authors.

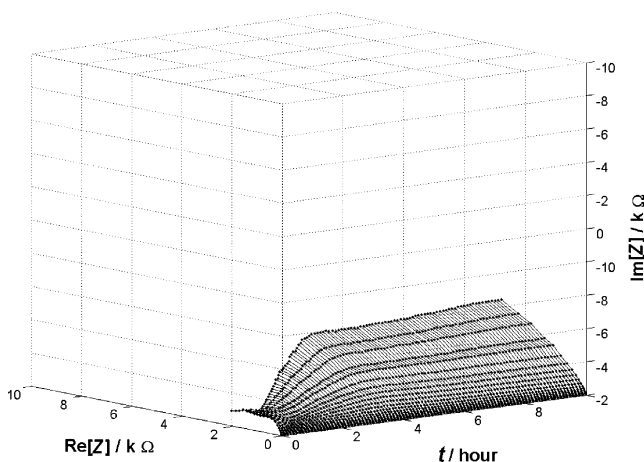


Fig. 1 DEIS result of Brass-MM55 without inhibitor in artificial seawater

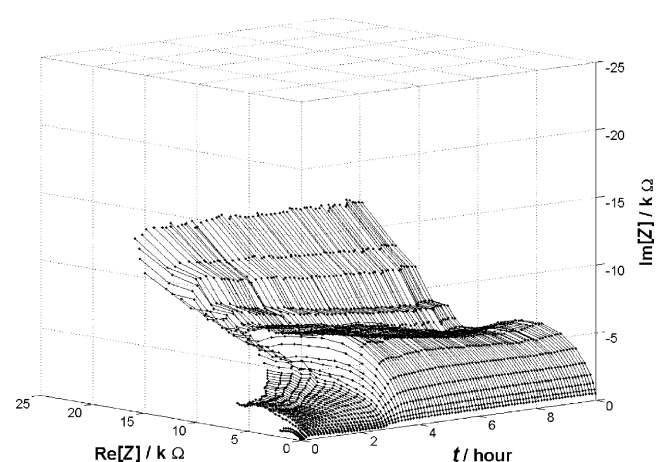


Fig. 3 DEIS result of Brass-MM55 with 0.0134 M BTA in artificial seawater

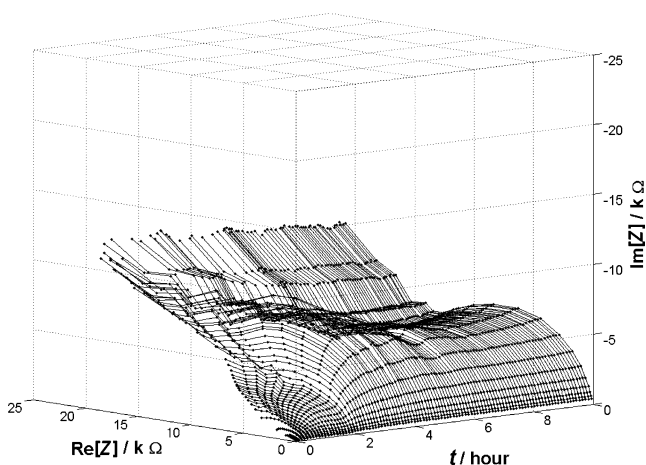


Fig. 4 DEIS result of Brass-MM55 with 0.0201 M BTA in artificial seawater

Experiment carried out by authors with use of DEIS technique in the range up to 4.5 kHz as the highest frequency. Obtained impedance spectra presented in the form of Nyquist plot contain only one time constant that evolve with time of experiment. Taking into consideration its character and variations in time of experiment authors decided to describe it by means of resistance and CPE bound with charge transfer process and electric double layer capacitance, respectively.

Changes connected with transport of reagents usually occur in the range of low frequencies (below Hz). In the case of the experiment carried out by authors, solution was under constant stirring which allows neglecting diffusion transport between surface and bulk of electrolyte. Impedance spectra obtained by means of classic impedance technique by other authors [32–34] manifest semicircle shape in the range of low frequencies; however, its

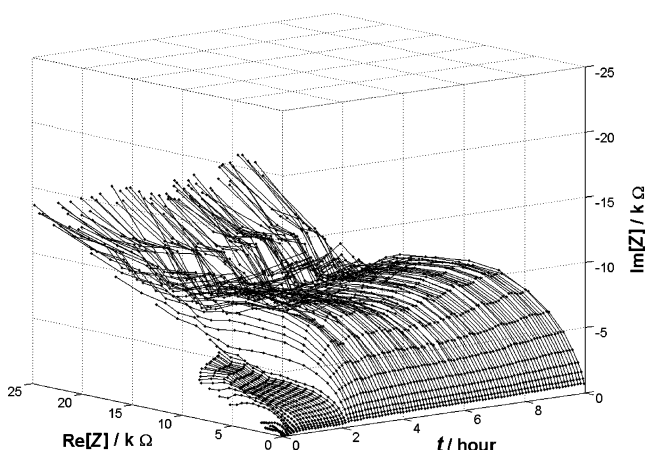


Fig. 5 DEIS result of Brass-MM55 with 0.0268 M BTA in artificial seawater

magnitude is too large to correspond to charge transfer resistance (kiloohms to megaohms). Such behavior can be explained with diffusion through the layer of finite thickness which, in authors’ case, is composed of oxides or other complex forms in the presence of BTA in the solution. Impedance of such diffusion is represented by equation below [30]:

$$Z_0 = \left[\tanh B(j\omega)^{1/2} \right] / Y_0(j\omega)^{1/2} \tag{2}$$

Where $B=l(D)^{1/2}$, D is the diffusion coefficient, l is the diffusion layer thickness, $Y_0=(\sigma(2)^{1/2})^{-1}$, and σ is the Warburg coefficient.

Lower frequency limit used in impedance measurement is 0.7 Hz. It is insufficient to detect complete range of diffusion. Taking into consideration the fact that changes in higher frequencies of diffusion process are identical for both finite diffusion for $\omega > 2/B^2$ as well as for classic Warburg impedance the latter element was used in the analysis. Warburg element was used only in terms of correct fitting procedure of other elements.

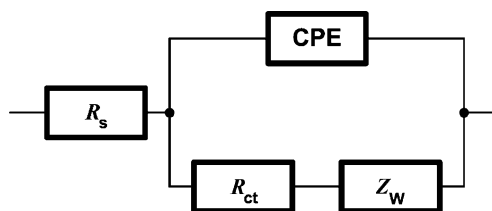
All impedance data were analyzed with ZSimpwin 3.1 program [35] with the use of electric equivalent circuit $R(Q(RW))$ introduced on Scheme 1. ZSimpwin exploits simple and efficient Down-Hill simplex method instead of popular Marquardt transformation during the fitting procedure. The measure of goodness of fit to model is χ^2 parameter, defined as:

$$\chi^2 = \sum_{i=1}^n \left[\frac{\left(Z'_i(\omega_i, \bar{p}) - a_i \right)^2}{a_i^2 + b_i^2} + \frac{\left(Z''_i(\omega_i, \bar{p}) - b_i \right)^2}{a_i^2 + b_i^2} \right] \tag{3}$$

where: ω_i , a_i , b_i —experimental data points, \bar{p} —parameters associated with a model, Z'_i , Z''_i —calculated point, during the analysis χ^2 did not exceed 1×10^{-4} attesting very high fit of received impedance spectra to proposed electrical equivalent circuit.

Key:

- R_s : resistance of electrolyte in bulk
- Z_W : Warburg impedance
- R_{ct} : charge transfer resistance at the metal surface
- CPE: constant phase element



Scheme 1 An electrical circuit of $R(Q(RW))$ model

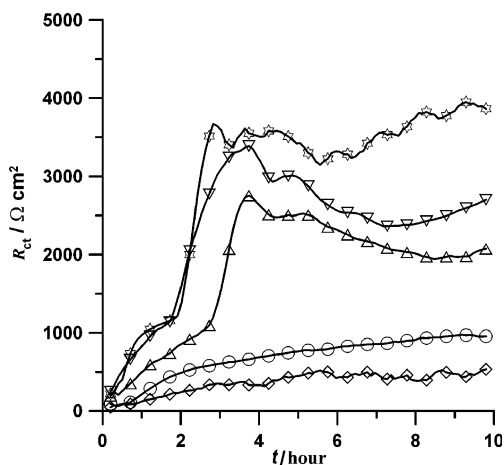


Fig. 6 R_{ct} change of Brass-MM55 in artificial seawater by using different concentration of BTA (\blacktriangledown 0.0268 M BTA, \triangleleft 0.0201 M BTA, \triangle 0.0134 M BTA, \circ 0.0100 M BTA, \diamond no inh.)

The impedance of constant phase element is given by

$$Z_{CPE} = [Q(j\omega)^n]^{-1} \tag{4}$$

Where Q describes the non-ideal behavior of the capacitance, j is the imaginary number, $\omega = 2\pi f$ is the angular frequency (rad/s), n is the exponent ($n < 0, 1 >$).

Figure 6 represents changes of charge transfer resistance of process, which converse might be used as a measure of electrode process rate.

Initial values of this parameter are similar and do not exceed $300 \Omega \text{ cm}^2$. For all of concentrations, the increase of R_{ct} is visible in the primary phase of exposition followed by its stabilization. Such behavior is a result of oxidation of material and simultaneous formation of surface layer. However, access to reaction surface is more difficult as the layer grows eventually leading to the inhibition of R_{ct} increase.

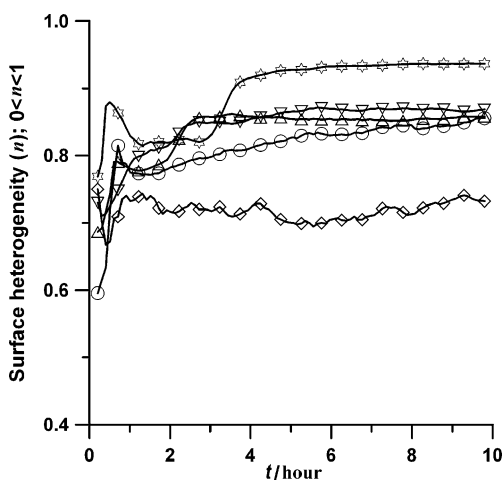


Fig. 7 Surface heterogeneity (n) value of Brass-MM55 in artificial seawater by using different concentration of BTA (\blacktriangledown 0.0268 M BTA, \triangleleft 0.0201 M BTA, \triangle 0.0134 M BTA, \circ 0.0100 M BTA, \diamond no inh.)

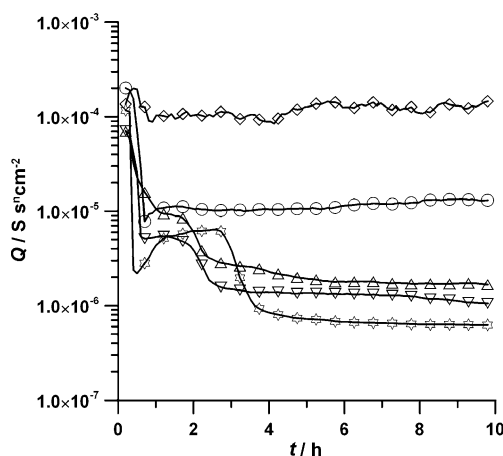


Fig. 8 Q parameter of the CPE element vs. time of exposure in artificial sea water in the presence of different concentration of BTA based on the DEIS results. (\blacktriangledown 0.0268 M BTA, \triangleleft 0.0201 M BTA, \triangle 0.0134 M BTA, \circ 0.0100 M BTA, \diamond no inh.)

Differences in R_{ct} values are visible depending on concentration of BTA used for the experiment, ranging from $\sim 400 \Omega \text{ cm}^2$ in case of lack of inhibitor up to $4 \text{ k}\Omega \text{ cm}^2$ for 0.0268 M of BTA. Such huge divergences are to be connected with properties of forming surface layer. In a solution containing only artificial seawater, one expects highly porous inhomogeneous layer of dozens of nanometers thickness whose main constituent is ZnO. Very thin homogeneous layer of few nanometers thickness is formed in the presence of BTA. It consists of Cu(I)BTA and Zn(II) BTA complexes [29].

In the case inhomogeneous electrode surface connected with surface roughness, porous layer etc. resultant impedance spectra exhibit the most often dispersion of time constants [36–38]. A measure of this dispersion is the deviation (decrease) of n parameter values. It allows identifying this parameter as magnitude of surface inhomogeneity. Figure 7 represents changes of n parameter during the experiment.

Similar as in case of charge transfer resistance increase of n parameter is visible in the primary phase of experiment resulting from the formation of outer layer on the surface.

Table 2 Inhibition efficiency values of BTA on Brass-MM55 in artificial seawater after 10 h

Concentrations	R_{ct} (Ohm cm^2)	Inhibition efficiency (IE%)
No inhibitor	501.8	–
0.0100 M BTA	969.4	48.24
0.0134 M BTA	2,088	75.97
0.0201 M BTA	2,736	81.66
0.0268 M BTA	3,830	86.89

Increase of inhibitor concentration in the solution consequences in obtaining results closer to the value of 1 which means that surface is more homogeneous. This is also confirmed by changes of Q parameter visible on Fig. 8.

Q parameter represents double layer capacitance occurring at the bottom of the pores [39, 40]. Taking this into consideration, as well as two rows of difference between no BTA in the solution and 0.0268 M BTA one can suggest fundamental influence of inhibitor concentration on reduction of pores size and/or quantity that are present in the outer layer.

The percentage inhibition efficiency (IE%) is calculated from the charge transfer resistance values [41] by using Eq. 5:

$$IE(\%) = \frac{(R_{ct})^{-1} - (R_{ct(inh)})^{-1}}{(R_{ct})^{-1}} \times 100 \quad (5)$$

Where $R_{ct(inh)}$ and R_{ct} are the charge transfer resistance values with and without inhibitors, respectively. Change of R_{ct} by the time is given in Fig. 6. Also, inhibition efficiency values are given in Table 2.

It is clear that the R_{ct} values increased in the presence of inhibitors. Also, the results obtained undoubtedly indicate that the investigated system was not in a stationary state. The change in spectra in Figs. 1, 2, 3, 4, and 5 confirms this idea. Figure 6 shows that inhibitor efficiency increased by the time but this was not in order. Changes of proposed equivalent circuit electric parameters, in particular R_{ct} , were very fast therefore dynamic EIS constitutes an attractive tool for investigation of such a non-stationary system.

Conclusions

The application of dynamic electrochemical spectroscopy technique to the corrosion protection by using inhibitor makes it possible to determine impedance changes as a function of time in the inhibition process. DEIS allows the investigation of inhibition process progressing in time. The changes of electrical parameters enable to determine when the system consists of metal inhibitor and aggressive medium is in the stable state. Studying inhibition effect of BTA for brass-MM55 in artificial seawater by DEIS shows that system reaches to stable state after 4 h. Thus, the calculated inhibition efficiencies should be more realistic when the system is in the stable state (e.g. at the end of 4 h). Result shows that BTA has excellent inhibition properties on the corrosion of brass-MM55 in artificial sea water. However, DEIS method is more informative since it gives information about time when BTA has stable maximum inhibition effect. Thus, measurements carried out with dynamic EIS seems to be more useful than classic EIS approach that base on frequency response analysis (FRA).

References

1. Stupnisek LE, Loncaric BA, Cafuk I (1998) *Corrosion* 54:713
2. Zaky AM (2001) *Br Corros J* 36:59
3. North RF, Pryar MJ (1970) *Corros Sci* 10:297
4. Quartarone G, Moretti G, Bellami T (1998) *Corrosion* 54:606
5. Rogers TH (1968) *Marine Corrosion Book*, George Newnes Ltd., London
6. ALSTOM Holdings DataBase. (2009) ALSTOM Power Sp zo.o. <http://www.alstom.com.pl/strona.php5?id=91>, Accessed 15 January 2009
7. Barbara R, Henryk K (1963) *Maly Poradnik Mechanika*, Wydawnictwa Naukowo-Techniczne, Warsaw
8. Asan A, Kabasakaloglu M, Işiklan M, Kılıç Z (2005) *Corros Sci* 47:1534
9. Sherif EM, Erasmus RM, Comins JD (2008) *Corros Sci* 50:3439
10. Babić-Samardžija K, Hackerman N (2005) *J Solid State Electrochem* 9:483
11. Costa JM, Luch JML (1984) *Corros Sci* 24:929
12. Dus B, Smialowska ZS (1972) *Corrosion* 28:105
13. Duprat M, Bui N, Dabost F (1979) *Corrosion* 35:392
14. Walker R (1973) *Corrosion* 29:290
15. Fox PG, Lewis G, Boden PJ (1979) *Corros Sci* 19:457
16. Costa SLFA, Agostinho SML (1989) *Corrosion* 45:472
17. Ashour EA, Sayed SM, Ateya BG (1995) *J Appl Electrochem* 25:137
18. Laz MM, Souto RM, Gonzalez S, Salvarezza RC, Ariva AJ (1992) *J Appl Electrochem* 22:1129
19. Wu X, Chou N, Lupher D, Davis LC (1998) *Conference on Hazardous Waste Research*, proceeding, Utah
20. Babić-Samardžija K, Metikoš-Huković M, Lončar M (1999) *Electrochim Acta* 44:2413
21. Youda R, Nishihara H, Aramaki K (1990) *Electrochim Acta* 35:1011
22. Kear G, Barker BD, Walsh FC (2004) *Corros Sci* 46:109
23. Sinyavskii VS, Kalinin VD (2005) *Prot Met* 41:317
24. Darowicki K, Orlikowski J, Lentka G (2000) *J Electroanal Chem* 486:106
25. Darowicki K, Slepki P, Szocinski V (2005) *Prog Org Coat* 52:306
26. Darowicki K, Gerengi H, Bereket G, Slepki P, Zielenski A (2006) (ISSN 1306-3588), *Korozyon*, pp. 3–9
27. Darowicki K, Orlikowski J, Arutunow A (2004) *J Solid State Electrochem* 8:352
28. Slepki P, Darowicki K, Andrearczyk K. *J Electroanal Chem* in press. Available from: doi:10.1016/j.jelechem.2009.05.002
29. Kosec T, Kek Merl D, Milošev I (2008) *Corros Sci* 50:1987
30. Mansfeld F, Han LT, Lee CC, Zhang G (1998) *Electrochim Acta* 43:2933
31. Mamas S, Kiyak T, Kabasakaloglu M, Koc A (2005) *Mater Chem Phys* 93:41
32. Nagiub A, Mansfeld F (2001) *Corros Sci* 43:2147
33. Ravichandran R, Nanjundan S, Rajendran N (2004) *Appl Surf Sci* 236:241
34. Ravichandran R, Nanjundan S, Rajendran N (2004) *J Appl Electrochem* 34:1171
35. AMETEK Princeton Applied Research DataBase (2009) *Electrochemical Softwares*, <http://www.princetonappliedresearch.com/products/Electrochemical.cfm>. Accessed 15 January 2009
36. Popova A, Christov M (2006) *Corros Sci* 48:3208
37. Growcock FB, Jasinski RJ (1989) *J Electrochem Soc* 136:2310
38. Lopez DA, Simison SN, Sanchez SR (2003) *Electrochim Acta* 48:845
39. Trachli B, Keddou M, Takenouti H, Srhiri A (2002) *Corros Sci* 44:997
40. Dermaj A, Hajjaji N, Joiret S, Rahmouni K, Srhiri A, Takenouti H, Vivier V (2007) *Electrochim Acta* 52:4654
41. Quraishi MA, Sardar R (2003) *J Appl Electrochem* 33:1163